Koistinen, Antti; Wang, Huaicheng; Hiltunen, Eero; Vuorinen, Tapani; Maloney, Thaddeus

Refinability of mercerized softwood kraft pulp

Published in:
Cellulose

DOI:
10.1007/s10570-024-05999-2

Published: 01/07/2024

Document Version
Publisher's PDF, also known as Version of record

Please cite the original version:
Koistinen, A., Wang, H., Hiltunen, E., Vuorinen, T., & Maloney, T. (2024). Refinability of mercerized softwood kraft pulp. *Cellulose*, *31*(10), 6471-6484. https://doi.org/10.1007/s10570-024-05999-2

Cellulose (2024) 31:6471–6484
https://doi.org/10.1007/s10570-024-05999-2

ORIGINAL RESEARCH

Refinability of mercerized softwood kraft pulp

**Antti Koistinen · Huaicheng Wang ·
Eero Hiltunen · Tapani Vuorinen ·
Thaddeus Maloney**

Received: 10 April 2024 / Accepted: 3 June 2024 / Published online: 8 June 2024

Abstract In this study, the impact of mercerization and PFI refining on the properties of softwood kraft pulp was investigated. Never-dried softwood kraft pulp was treated with 15 wt% NaOH to generate highly hydrated fibers, followed by PFI refining to increase pulp fibrillation and porosity. The original and modified pulp properties were assessed for morphological and chemical composition. Differential scanning calorimetry (DSC) tests and water retention value (WRV) measurements were conducted to evaluate pulp swelling behavior and porosity. Fiber bonding potential and strength properties were evaluated from handsheets of mercerized and unmercerized pulp. Mercerization with 15 wt% NaOH successfully converted cellulose I to cellulose II, leading to slightly increased pulp swelling and micropore volume. However, the mercerization reduced handsheet strength properties. Furthermore, PFI refining resulted in a negligible enhancement of bonding in mercerized pulp, in stark contrast to its significant effect on unmercerized kraft pulp.

Keywords Kraft pulp · Mercerization · Porosity · Tensile properties · Swelling

A. Koistinen (✉) · H. Wang · E. Hiltunen · T. Vuorinen · T. Maloney
Department of Bioproducts and Biosystems,
School of Chemical Engineering, Aalto University,
Aalto FI-00076, Finland
e-mail: antti.koistinen@aalto.fi

Introduction

When kraft pulp fibers are treated with strong alkali, the cellulose swells and partially dissolves (Sobue et al. 1939; Isogai and Atalla 1998; Cuissinat and Navard 2006; Kihlman et al. 2013; Zhang et al. 2013). Upon subsequent precipitation caused by neutralizing in acid or washing with water, the cellulose is converted to a mixture of amorphous cellulose and cellulose II and the morphology of the fiber is greatly changed. Such "mercerized pulps" have several current commercial applications, e.g., filter paper production and nonwovens (Lund et al. 2012; Liu et al. 2015), but could have potential wider applications if we learn to modify and control the fiber structure. It is important to gain more information how mercerized pulps respond to mechanical refining. Furthermore, the effect of alkali on pulp fiber structure and fibrillation is relevant to mechanisms at play in pulp dissolution for producing regenerated cellulose textile fibers. Fibers which are exposed to alkali may, under certain conditions, gelate or hornify thus inhibiting further dissolution (Korhonen and Budtova 2019; Reyes et al. 2022).

Cellulose has a complex structure that can be characterized on three levels (Krässig 1993): molecular, aggregate, and morphological level. On molecular level, cellulose is a linear polymer, composed of (1–4) bonded β-D-glucopyranosyl units, characterized by its molecular size distribution and degree of polymerization (DP). Cellulose molecules form intra- and intermolecular interactions via the hydrogen bonding of the hydroxyl groups and van der Waals forces (Wohlert et al. 2022). These interactions contribute to the organization of cellulose on a supramolecular level, leading to the aggregation of individual cellulose polymers into ordered crystalline regions and less ordered amorphous regions. This organization results in a combination of structured crystalline areas and unstructured amorphous areas withcellulose. In natural fibers, the cellulose chains are often oriented along the fiber axis, either in parallel or antiparallel arrangement. Finally, the elementary fibrils form the morphological architectures ranging in the macroscopic domain, encompassing the structure of the cell wall in natural plant fibers, skin-core characteristics of regenerated cellulose filaments, and the porosity of cellulose in measured in nanometers to micrometers.

Due to the hydroxyl groups present in the cellulose β-D-glucopyranosyl units, cellulose not only forms intra- and intermolecular hydrogen bonds with cellulose molecules but also surrounding water molecules. Cellulosic materials are strongly hydrophilic, and this property is crucial for many cellulose-based products. The water-bounding properties of cellulose may be tailored. A common method widely used in the textile industry for cotton fiber water accessibility increase is mercerization, a method named after John Mercer in 1850. The process involves treating cotton with strong sodium hydroxide (NaOH). The method improves cotton properties, improving its dye affinity and tensile strength. Later research has shown that concentrated NaOH introduces changes to cellulose on all three architectural levels: cellulose fibers swell, and the ordered, crystalline structures become disorganized, forming alkali cellulose. Swelling can be observed also at microfibrillar level (Eronen et al. 2009). As the singular cellulose molecules are liberated due to loss of crystallinity, the reactivity of cellulose increases upon alkaline treatment via increasing the hydroxyl group accessibility. If the alkali penetrating the fibers is washed away, the cellulose recrystallizes into cellulose II – a cellulose crystalline allomorph absent in higher plants, but synthesized by some bacterial and algal species (Sisson 1938; Hirai et al. 1997) – accompanied with amorphous cellulose (Halonen et al. 2013).

The crystalline unit cell of cellulose II is slightly larger than that of cellulose Iβ, with volumes of 671.3 $Å^3$ and 658.3 $Å^3$, respectively (Langan et al. 2001; Nishiyama et al. 2002). Additionally, the c-axis spacing is larger in cellulose Iβ (10.38 Å) compared to cellulose II (10.31 Å), indicating that the cellulose II has even more lateral space than suggested by the total volume difference alone. However, the volume difference between cellulose I and II is 13 $Å^3$, whereas one water molecule is roughly 30 $Å^3$. In the hydrated state, the hydrated cellulose II exhibits 8.5% larger crystalline unit cell compared to non-hydrated cellulose II (Wada et al. 2010). This larger unit cell in hydrated state provides more accessible chemical architecture, making hydrated cellulose II more reactive in various chemical reactions, such as oxidation (Pönni et al. 2014) and enzymatic hydrolysis (Wada et al. 2010). Conversely, dewatered and dried cellulose II forms a denser fibril network resistant to dissolution (Ngene et al. 2022).

In addition to changing the crystalline allomorph, alkaline treatments are known to dissolve hemicelluloses present in pulp. NaOH is utilized in both cold caustic extraction (CCE) and hot caustic extraction (HCE) kraft pulp purification to produce dissolving grade pulp (Schild and Sixta 2011). The aim of hemicellulose removal is to increase cellulose purity that is necessary for cellulose dissolution in production of regenerated cellulose products. Previous research has shown CCE treatments may increase reactivity via removal of hemicelluloses (Dou and Tang 2017), however, opposite may also occur, as some molecular weight hemicelluloses act as spacers between cellulose microfibrils, enabling solvent accessibility to the cellulose fibers (Gehmayr et al. 2012). Upon spacer hemicellulose removal, cellulose microfibrils form hydrogen bonds, causing an irreversible loss in porosity, ultimately decreasing cellulose reactivity in dissolution. Thus, mercerization is a process useful for improving cellulose reactivity in certain end-uses, however, in certain applications the alkaline treatment has an adverse effect on the reactivity.

An alkaline treatment affects swelling and swellability of fibers. In our recent work, we treated softwood kraft pulp with a NaOH/ZnO solvent using a freeze-thawing treatment, which increased the hydrated pore volume over 100% (Koistinen et al. 2023), indicating significant swelling after an alkaline treatment. However, the treatment effect on bonding properties was uninvestigated.

Refining is a mechanical modification of pulp fibers that aims to improve the properties of the pulp fibers in paper of board manufacturing. During refining, the fiber characteristics change in terms of shortening the fibers, introducing fines, straightening the fibers, removing external parts of the cell wall, and causing external fibrillation. The mechanical properties of pulp fiber networks improve, reflected in elevated tensile properties and drainage resistance, whereas bulk decreases.

In this study, we treated never-dried softwood kraft pulp with 15 wt% sodium hydroxide to mercerize and swell it into a cellulose II hydrate. Our aim was to preserve most of the hemicelluloses after mercerization by neutralizing the alkali using acid. The hypothesis was that the cellulose swelling would increase, ultimately increasing the interfibrillar bonding capacity via increased hydrogen bonding between individual cellulose molecules and cellulose fibers. The goal was to assess the bonding capacity of the hydrated pulp in forming cellulose fiber networks. To enhance the bonding capacity, the hydrated pulp was treated with PFI refining. The pore and swelling properties of the pulp as well as structural carbohydrate composition was determined. The pore structure was assessed both using conventional water retention value (WRV) method and thermoporosimetry. We assessed the bonding capacity of the mercerized pulp in handsheets and testing them for mechanical properties.

Materials

Never-dried bleached softwood kraft pulp (BSK) from a Finnish pulp mill was used to examine the effect of alkaline treatment on pulp bonding and swelling properties. To produce mercerized kraft pulp (M-BSK), BSK was treated with aqueous sodium hydroxide (NaOH). The treatment was carried out by mixing aqueous NaOH solution and BSK to form a 10 wt% pulp and 15 wt% NaOH solids content mixture. The mixture was closed in an airtight container in for 60 min in room temperature (~23 °C). Then, excess NaOH was extracted in a Büchner funnel, and the mixture was diluted to ca. 3 wt% solids content with deionized water. The sample was neutralized with 1 M sulfuric acid until ca. pH 5.5. Finally, the pulp was washed with deionized water until its conductivity was below 50 µS/cm. Total of 200 g bone dry pulp was treated in two consecutive batches that were combined.

The BSK and M-BSK structural carbohydrate composition was analyzed following the method by Sluiter et al. (2011). Prior to analysis the samples were dried in atmospheric conditions and milled. The instrument used was Dionex ICS-3000 system (Thermo Fischer Scientific, US), which utilized the high-performance anion exchange chromatography with pulsed amperometric detection (HPAEC-PAD) method. The measurement was performed in duplicate for each sample. The Janson formulae (Janson 1970) were applied for calculating the cellulose and hemicellulose content from the monosaccharide constituents.

To evaluate sample crystalline allomorph, BSK and M-BSK were analyzed with Renishaw inVia™ confocal Raman spectroscope (Renishaw, United Kingdom), equipped with 2400 1/mm grating, 20× lens, and 532 nm wavelength laser. Integration time of 0.5 s and 200 number of accumulations were used. The collected spectra were baseline corrected and normalized to range from 0 to 1 in intensity (largest intensity at 1096 cm^{-1}) using Renishaw Wire 5.3 software.

For studying drying-induced hornification, BSK and M-BSK were dried at 105 °C and rehydrated in deionized water.

Methods

The BSK and M-BSK pulps were cold disintegrated following ISO 5263-1 and refined using a PFI-Mill 60 (Hamjern AS, Norway) in accordance with TAPPI T 248 method. 30 g (oven dry basis) of sample was treated with 100, 200, 400, 800, and 1600 revolutions.

The fiber dimensions and other morphological characteristics were measured using an ISO 16065-2 compliant Valmet Fiber Image Analyzer FS5 (Valmet Oyj, Finland).

The total cell wall pore volume was measured by centrifugation as the water retention value (WRV) according to ISO 23714:2014 standard.

Fiber pore size distribution (PSD) was measured with thermoporosimetry. The method is based on the water melting point depression of molecules enclosed in cavities in the pulp cell wall. The pore diameter (D)

and the melting point depression (ΔT_m) has a correlation following the Gibbs–Thomson equation, which has the simplified expression:

$$D = \frac{k}{\Delta T_m}, \tag{1}$$

where k is a constant earlier determined to equal 43 K·nm (Maloney 2015). Using a Mettler Toledo DSC3+ (Mettler Toledo, Switzerland), the PSD were determined from samples controlled to a moisture content of 1.5 g H_2O/g fiber. A small fiber amount (ca. 5 mg) was weighed to an aluminum sample pan, which was sealed and weighed. The DSC was equipped with an autosampler. The PSD is determined from a freezing exotherm under non-supercooling conditions in the range −0.2 to −20 °C. The DSC temperature calibration was performed utilizing mercury and distilled water; enthalpy calibration was done with distilled water. Assuming a cylindrical pore geometry, the pore surface area was calculated in the mesoporous range and extrapolating to 0.28 nm pore size in the nanopore range using a double log-normal model distribution. The pore volumes are categorized as micropores ($D < 2$ nm), mesopores ($2 < D < 50$ nm) and macropores ($D > 50$ nm). Macropores are outside the range of thermoporosimetry, thus the macropore volume is calculated as:

$$V_{\text{macropore}} = WRV - V_{\text{micropore}} - V_{\text{mesopore}}. \tag{2}$$

More detailed method description is available elsewhere (Maloney and Paulapuro 1999; Maloney 2015; Koistinen et al. 2023).

To examine internal fibrillation qualitatively, a Simons' staining was performed on samples (Yu et al. 1995). Following a method reported by Akhtar et al. (1995), 1 w% aqueous Pontamine sky Blue 6BX and 1 w% aqueous Sun yellow dye solutions were prepared from dry powder (from abcr GmbH, Germany) and mixed in a 1:1 ratio. On a microscopy glass slide, a small fiber sample was flooded with the dye. The sample slide was placed in an oven at 60 °C until dye evaporation. A cover glass was placed on the sample and the excess stain dye was rinsed with deionized water. Finally, the sample was studied with a Leica DM750 microscope.

Handsheets were produced from refined BSK and M-BSK, and non-refined reference pulps. Following ISO 5269-1 method, 80 g/m^2 grammage handsheets were prepared using a sheet mold model FI 101 (Lorentzen & Wettre, Sweden) with deionized water. Handsheets were pressed following the standard and dried in a drum dryer (model FI 119, Lorentzen & Wettre, Sweden) at 65 °C for two hours. Sheets were stored in 23 °C and 50% relative humidity for at least 24 h prior analysis.

The tensile properties of handsheets were analyzed with Tensile Tester model SE 064 (Lorentzen & Wettre, Sweden), and for brittle handsheets, MTS 400 (MTS Systems Norden, Sweden) tensile and compression testing device was used, following ISO 1924-3. Handsheet thickness was analyzed with Thickness Tester model SE 250 (Lorentzen & Wettre, Sweden) to calculate density and bulk following ISO 534. Sheet grammage was determined according to ISO 536. Sheet internal bonding was determined with Huygen internal bond tester model G411 (Huygen Corporation, USA) following TAPPI T569. Zero span strength was analyzed with Z-Span 1000 zero span tester (Pulmac Systems, USA) in accordance with ISO 15361.

Results and discussion

Chemical composition and mercerization

Previous research has shown that alkaline treatment causes changes in cellulose morphology, crystalline structure, and swelling capacity (Chen et al. 2016; Friebel et al. 2019; Li et al. 2019). The aim of our treatment was to try to preserve as much of hemicelluloses in the kraft pulp as possible via neutralizing the alkali prior washing with deionized water; method where kraft pulp is modified with alkali in near-room-temperature is often referred to as cold caustic extraction (CCE). The goal in CCE is converting kraft pulp to dissolving grade pulp via removal of hemicelluloses, which also affects the porosity (Dou and Tang 2017).

Hemicelluloses are known to contribute to interfibrillar bonding (Pere et al. 2019), and NaOH treatments are known to dissolve hemicelluloses from pulp, thus the carbohydrate composition prior and after alkaline treatment was examined. Our mercerization affected hemicelluloses, assuming arabinose being a part of xylan, causing 36% of xylan and 13% of glucomannan o solubilize. All cellulose is assumed to retain in the fibers. The glucomannan retention of 87% reflects its sustantial resistance to NaOH solubilization. The data shows stability of hemicellulose components in alkaline conditions.

Cellulose arranges in ordered crystalline domains and swelling in aqueous alkaline solvents causes the cellulose crystallinity to change; dissolution in aqueous alkali requires the crystalline structures of cellulose to break and individual cellulose chains to liberate from their inter- and intramolecular hydrogen bonds. The ordered crystalline domains may be detected with methods such as X-ray diffraction (XRD) or Raman spectroscopy. XRD is a more common method for crystallinity analysis in soft materials. Raman-based methods, as well as FT-IR and NMR based crystallinity methods, determine the crystallinity by measuring spectral features affected by crystallinity. In Raman, cellulose I and II crystallinities are represented by peaks positioned at 380 and 577 cm^{-1}, respectively (Agarwal et al. 2010, 2021). We collected Raman spectra from BSK and M-BSK to analyze the allotropic conformation and crystallinity of cellulose, represented in Fig. 1. In BSK, a clear peak is visible at 380 cm^{-1}, which upon alkaline treatment disappears, and a distinct peak appears at 577 cm^{-1}; The 577 cm^{-1} peak is only present in cellulose II (Agarwal et al. 2021), thus, the alkaline treatment changed the crystal form to cellulose II, which is present in regenerated and mercerized cellulose. Earlier studies showed that mercerization and the regeneration of dissolved cellulose led also to a reduced crystallinity, indicating amorphous cellulose formation (Azubuike et al. 2012; Jin et al. 2012; Yue et al. 2013; Han et al. 2013; Ji et al. 2018), resulting in cellulose II with higher amorphous cellulose content than the original cellulose I.

Fiber dimensions and pore characteristics

Table 2 shows the fiber dimensions and other fiber characteristics for BSK, M-BSK, and PFI refined samples; Fig. 2 displays microscopy images of BSK, M-BSK, and their states after 1600 PFI revolutions. As a result of refining, the unmercerized fiber length was about constant in the range 1.74–1.77 mm. Fibrillation increased as a function of refining revolutions, which is an expected result. Kinks decreased slightly, fiber curl was about constant, fines increase from 11.4 to 13.9%.

A dramatic change was introduced from alkaline treatment: comparing the M-BSK to BSK, the alkaline treatment caused the fibers to curl and kink extensively. The external fibrillation of the fibers increased, and fines were generated. Similar effect from alkaline treatment has been reported (Ji et al. 2018; Pere et al. 2019; Dias et al. 2019). The fiber length decreased from mercerization by 38%, fiber width increased slightly. During alkaline treatment, the ribbon-like

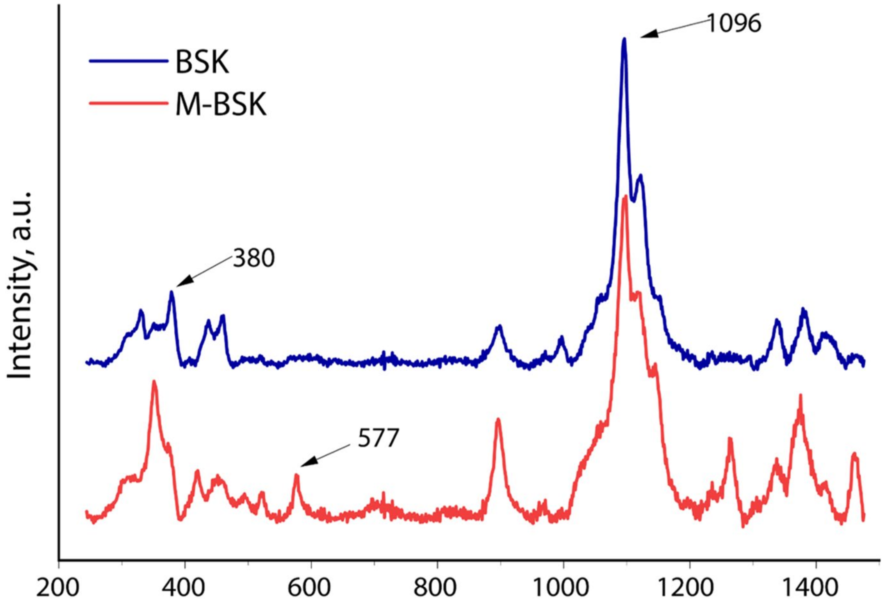

Fig. 1 Raman spectra for BSK and M-BSK. 380 cm^{-1} and 577 cm^{-1} peaks are characteristic for cellulose I and II, respectively; the occurrence of 1096 cm^{-1} is independent of cellulose crystallinity

Fig. 2 BSK and M-BSK microscope images. **a** BSK, **b** 1600 PFI revolutions BSK, **c** M-BSK, **d** 1600 PFI revolutions M-BSK

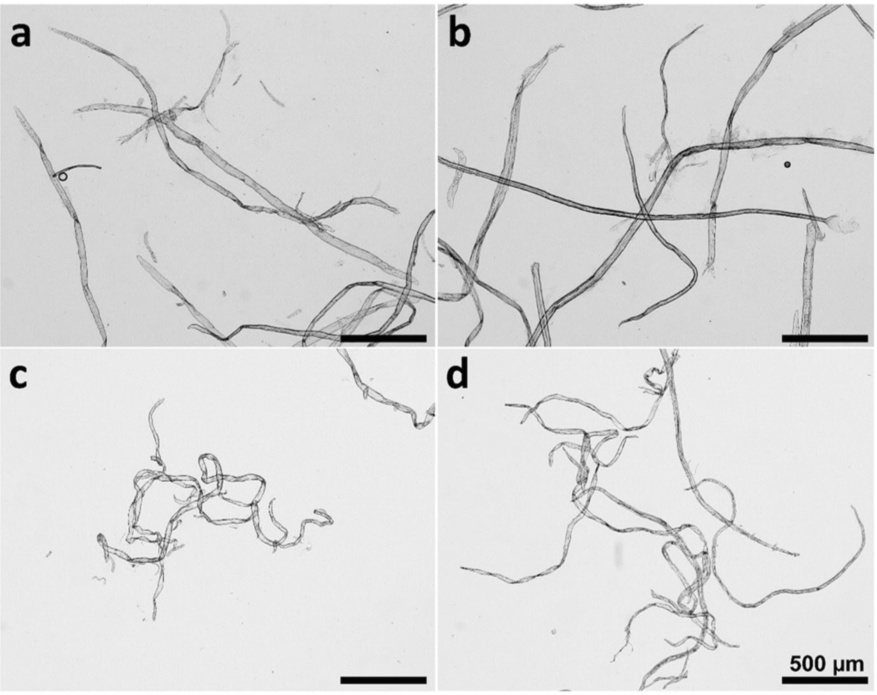

pulp fibers convert into swollen tubular morphology, or heterogeneously experience ballooning-type swelling, and simultaneously shrink in length. (Choi et al. 2018; Le Moigne et al. 2010; Zhang et al. 2013). However, length decrease of this magnitude was unexpected: earlier studies have shown a 12–15% decrease in fiber length (Lund et al. 2012; Liu et al. 2015; Choi et al. 2016), caused by swelling (Choi et al. 2016). A possible explanation for current result is a measurement error due to the curliness of the mercerized fibers: when curling in the detector optical plane, the optical fiber length measurement systematically reports the fiber lengths shorter. In an earlier study, alkaline treatment was used for extracting hemicelluloses from kraft fibers (Lund et al. 2012), and subsequent PFI refining caused the curliness to reduce slightly. It is note-worthy that during refining, the external fibrillation of mercerized pulp was reduced from 0.29 to 0.14%. It appears the refining blades scraped fibrils off the fiber surface, without generating more fibrillation. This is the opposite effect as unmercerized pulp, where the attrition of the outer cell wall raises fibrils on the fiber surface.

Figure 3 shows that the water retention value (WRV) increased from the alkaline treatment. The increase is small, nevertheless significant, and shows an increase in porosity from the mercerization. This can be attributed to the expansion of the small interior pores of the fibers and fibrils resulting from the alkaline treatment (Ji et al. 2018). Furthermore, mercerization introduces disordered amorphous cellulose at high NaOH concentrations, leading to lower total crystallinity and higher WRV (Halonen et al. 2013).

For BSK, the WRV increased with higher PFI refining revolutions. This was an expected result: the refining partially removes the outer layers of the cell wall and ruptures internal bonds in the S2 layer. Consequently, the pulp fibers can absorb more water and swell after PFI refining (Page 1989). The combination of internal and external fibrillation is the primary cause of increased bonding in chemical pulp due to refining.

In contrast, for alkali treated pulp, the WRV slightly decreased as a function of PFI refining revolutions. Obviously, the alkali treatment of the fibers partially dissolved the cellulose and caused a substantial reorganization of the cell wall architecture. Effectively, this process physically crosslinks the fibrils, so that even with significant mechanical treatment the cell wall layers do not split and internally fibrillate. Thus, the fibers do not swell with refining, at least with the type of pulp and refining degree used here.

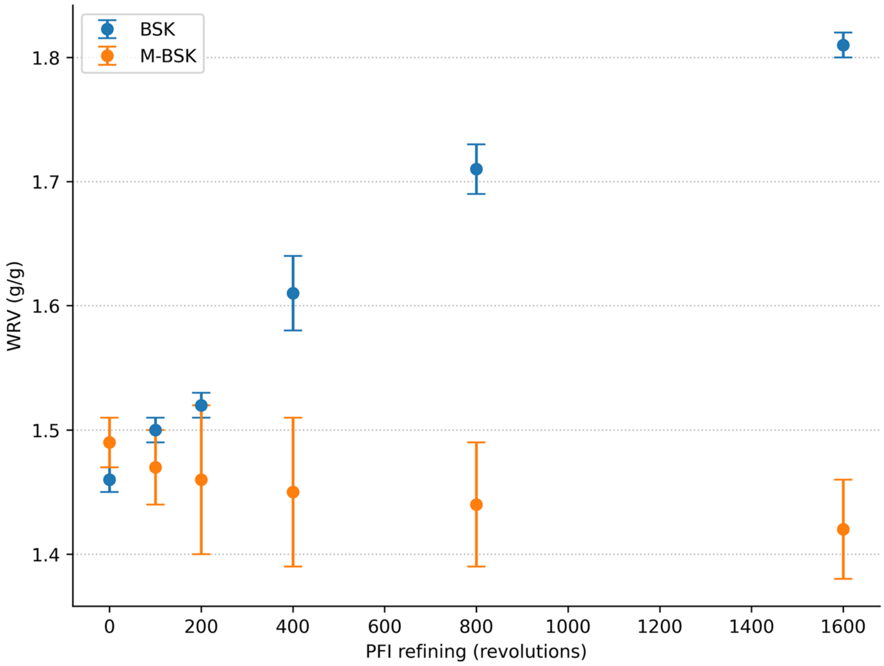

Fig. 3 Water retention values for unrefined and refined BSK and M-BSK

Table 1 Carbohydrate composition of BSK and M-BSK

Sample	Cellulose (%)	Xylan (%)	Glucomannan (%)	Total Hemicelluloses (%)
BSK	81.5	9.8	8.2	18.0
M-BSK	86.1	6.3	7.1	13.4

Treatment with high concentrations of alkali (> 10 w%) can lead to a reduction in water retention value (WRV) as a result of hemicellulose loss, given that hemicelluloses are capable of absorbing significant quantities of water. However, as demonstrated in Table 1, the loss of hemicellulose was slight. Consequently, the increase in porosity and the reduction in cellulose crystallinity play a more significant role in the enhancement of WRV in samples treated with alkali.

Refining normally causes fibers to delaminate on the fiber surface. It appears that mercerized pulp is fibrillated (Table 2), seen as an increase in external fibrillation, and this is reversed by the refining, which causes the porosity loss measured in WRV.

The internal fibrillation can be measured by considering changes to the pore size distributions (PSD) of cell wall pores. In Table 3 we have divided the pore volumes into macro-, meso- and micropores. Surface areas, calculated from the PSD in the micropore and pores regimes are also included in the table. When unmercerized kraft pulp is refined, the compressive and shear forces cause separation and delamination of cell wall layers (Chen et al. 2013). There is also some splitting of fibril aggregates and finer scale structures, especially in the initial phase of refining. This is reflected in the large increase in mesopore volume, and thus, mesopore volume increases from 0.67 to 0.88 mL/g and the meso-scale surface area from around 370 to 580 m^2/g (Table 3) over the range of the experiment. Micropores are pores less than 2 nm; this class of pores is highly related to the amount of amorphous cellulose or hemicellulose present. This was not affected by the refining within the range of this experiment.

However, mercerization does increase the amount of amorphous cellulose, which increases the amount of non-freezing water and micropore water (Ji et al. 2018), which are related quantities. Thus, mercerization increases the microscale surface area from 1060 to 1390 m^2/g. When mercerized pulp is refined there is virtually no increase in macropore, mesopore or micropores volume; this is also reflected in surface area distributions plotted in Fig. 4, where M-BSK and M-BSK refined with 1600 revolutions distributions

Table 2 Fiber morphology of unrefined and refined BSK and M-BSK

Sample	Length[1] (l) (mm)	Fiber width (µm)	Fibrillation[2] (%)	Kink (1/m)	Curl (%)	Fines[3] (%)
BSK	1.74	28.3	0.07	4320	15.3	11.4
BSK-100	1.73	28.2	0.08	3930	14.3	11.8
BSK-200	1.70	28.1	0.09	3840	14.3	12.7
BSK-400	1.77	28.0	0.09	3730	12.5	12.3
BSK-800	1.70	28.3	0.11	3680	15.1	12.7
BSK-1600	1.70	28.8	0.18	3620	15.1	13.9
M-BSK	1.08	28.9	0.29	9180	36.7	14.4
M-BSK-100	1.18	28.8	0.27	8790	35.4	13.2
M-BSK-200	1.26	28.1	0.18	8270	34.0	13.2
M-BSK-400	1.18	28.8	0.24	8430	33.5	15.4
M-BSK-800	1.14	28.0	0.21	8370	34.2	17.9
M-BSK-1600	1.31	27.3	0.14	7500	32.2	14.5

[1] Length-weighted average fiber length. [2] Projection area of fibrils in relation to the projection area of the entire object, scaled into a percentage. [3] Fines as a percentage of arithmetic distribution

Table 3 Pulp pore properties

Sample	Non-freezing water (mL/g)	Macropore volume (mL/g)	Mesopore volume (mL/g)	Micropore volume (mL/g)	Total hydrated surface area (m^2/g)	Mesopore surface area (m^2/g)	Micropore surface area (m^2/g)
BSK	0.25 ± 0.04	0.56	0.67 ± 0.04	0.23 ± 0.01	1430 ± 140	370 ± 30	1060 ± 100
BSK-100	0.29 ± 0.03	0.48	0.75 ± 0.04	0.27 ± 0.01	1750 ± 90	460 ± 30	1280 ± 80
BSK-200	0.26 ± 0.01	0.34	0.89 ± 0.03	0.28 ± 0.01	1770 ± 30	640 ± 20	1140 ± 40
BSK-400	0.24 ± 0.03	0.54	0.82 ± 0.02	0.25 ± 0.01	1580 ± 50	560 ± 30	1020 ± 60
BSK-800	0.24 ± 0.03	0.62	0.86 ± 0.02	0.24 ± 0.01	1530 ± 30	590 ± 20	940 ± 40
BSK-1600	0.27 ± 0.05	0.69	0.88 ± 0.06	0.25 ± 0.02	1620 ± 70	580 ± 50	1030 ± 80
M-BSK	0.33 ± 0.04	0.40	0.79 ± 0.05	0.29 ± 0.02	1860 ± 200	470 ± 40	1390 ± 130
M-BSK-100	0.39 ± 0.02	0.36	0.77 ± 0	0.34 ± 0	2040 ± 0	460 ± 0	1570 ± 0
M-BSK-200	0.39 ± 0.03	0.34	0.76 ± 0.01	0.36 ± 0	2140 ± 20	460 ± 10	1680 ± 20
M-BSK-400	0.36 ± 0.03	0.30	0.82 ± 0.06	0.33 ± 0.02	2040 ± 180	500 ± 40	1540 ± 130
M-BSK-800	0.35 ± 0.01	0.31	0.81 ± 0.03	0.32 ± 0.01	2020 ± 90	500 ± 20	1520 ± 70
M-BSK-1600	0.33 ± 0.09	0.33	0.79 ± 0.02	0.3 ± 0.01	1910 ± 80	490 ± 20	1430 ± 60

Mesopore range includes pores with diameter $50 > D > 2$ nm, micropores diameters $D < 2$ nm

are identical. This suggest that the internal structure of the cell wall is completely swollen and fused. The original structure of aligned microfibrils has been altered to highly intercalated structure of amorphous cellulose and localized cellulose II crystallites. This structure does not undergo any meaningful swelling from mechanical refining at these energy levels. Due to high number of kinks and fiber curl, fiber bonding is limited, and the inability to fibrillate internally and externally inhibits developing bonding capability during refining. Oven drying led to hornification of both mercerized (WRV 0.89 ± 0.04 g/g) and non-treated samples (WRV 0.90 ± 0.01 g/g), seen as WRV decrease of 0.6 g/g after rehydrating the dried samples.

Simons' staining

Simons' staining serves as a rapid qualitative technique to elucidate the internal fibrillation of pulp by employing dyes to indicate the size of pores within the fiber cell walls. This method utilizes a dye with small dye molecules, such as Pontamine Sky Blue 6BX, that penetrate small pores, and larger high

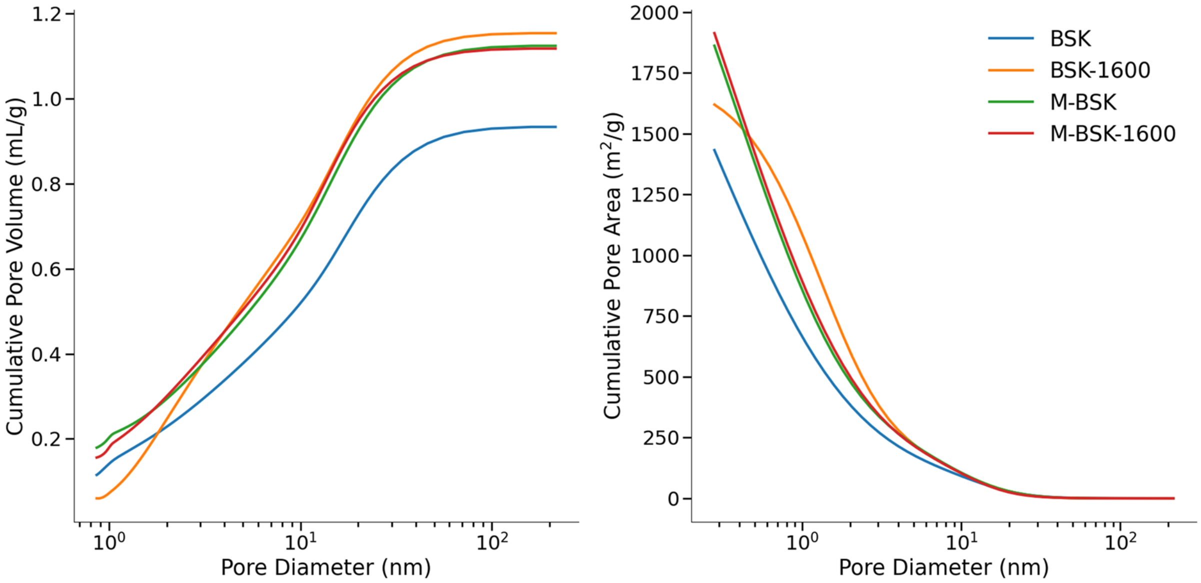

Fig. 4 Cumulative pore volume and surface area for unrefined and refined pulp (1600 revolutions), BSK and M-BSK

molecular weight dye, in this case, Sun Yellow, which are too large to enter and thus remain on the fiber surfaces. The original yellow azo-stilbene dye used by Simons, Direct Orange 15 (C.I. 40,002/40,003) production has been discontinued; however, a suitable alternative has been discovered in Direct Yellow 11 (C.I. 40,000) (Kwok et al. 2017), that is also known by its trade name Sun Yellow.

When fibers lack large pores, they retain the blue dye, indicating smaller pore sizes. Conversely, larger pores can accommodate the high molecular weight yellow dye, resulting in fibers appearing yellow due to the stronger affinity of the larger dye molecules. Notably, the yellow dye displaces the blue dye in accessible larger pores. If all pores are smaller than the Stokes diameter of the yellow dye, the fibers will remain blue, highlighting the method's ability to visually differentiate between fibers based on the presence and size of internal pores (Yu et al. 1995). This approach provides insights into the fiber's pore structure, crucial for understanding and optimizing cellulose dissolution and interaction in NaOH-water systems.

In Fig. 5a, many of the never dyed, unmercerized, unrefined fibers are yellow, but some fibers, and regions within fibers, have a tighter pore size distribution and remain blue. When refined (Fig. 5b), the fraction of yellow fibers increases as the cell wall is delaminated and the pulp swells. When mercerized, the pulp becomes completely blue (Fig. 5c), indicative of the internal gelation of the cell wall described earlier. When refined, the mercerized pulp does not become yellow as internal fibrillation does not happen for this pulp (Fig. 5d). When unmercerized pulp is dried and rewetted (hornification) pores are closed and the pulp becomes blue in Simons' staining (Fig. 5e) (Hult et al. 2001). Sometimes alkali treatment of pulp is described as hornification although this process is rather different than the loss of swelling when ordinary low yield pulp is dried and rewetted. In that case, the fibrils aggregate in drying, but the cell wall swelling can be regenerated by mechanical refining. However, when pulp is mercerized, the structure of the cell wall hornifies in such a way that it cannot be swollen by ordinary refining. Furthermore, the Simons' staining patterns (Fig. 5) do not completely correlate with the pore size distributions measured by thermoporosimetry (Fig. 4): thermoporosimetry indicates that M-BSK has more large pores than BSK, but the M-BSK stain remains blue, indicating absence of large pores capable of retaining the yellow dye. In conclusion, mercerized cellulose has a lower pore accessibility compared to unmercerized pulp.

Simons' staining was proven to be a useful method for assessing pulp porosity changes. However, more

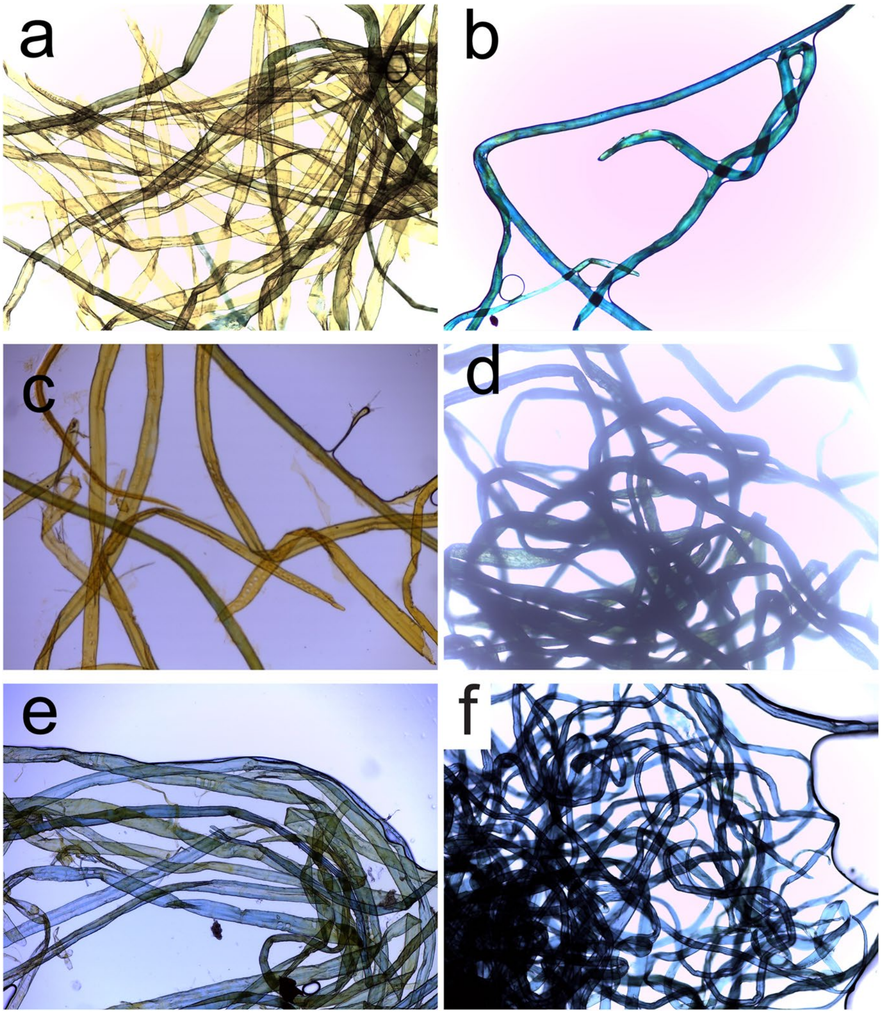

Fig. 5 Simons'-stained samples. **a** Unrefined, **c** refined, and (**e**) hornified BSK. **b** Unrefined, **d** refined, and (**f**) hornified M-BSK

accurate results could be achieved by determining exact dye molecular sizes via gel permeation chromatography.

Handsheet properties

The refined BSK and M-BSK were formed into handsheets to quantify bonding and strength properties. The results are shown in Fig. 6. Unmercerized pulp has some bonding capacity, which is greatly increased by refining. Fibers swell and become more flexible, external fibrils and fines are generated, all of which increase bond area and bond strength. This causes bulk to decrease as bonding and strength increases. Fiber strength, as reflected in the zero-span test, is not much affected by refining. These effects are well known and have been described in numerous publications (Wang et al. 2005; Koskenhely 2008; Gharehkhani et al. 2015).

Mercerization reduced the tensile index to almost zero, which indicates the fibers lack virtually any bonding capacity. This is also seen in the low internal bond strength of the mercerized sheets. The low bonding can be partially explained by the lower hemicellulose content and the curly morphology of the mercerized pulp. However, such low bonding indicated that the amorphous/cellulose II generated in mercerization, has itself very low bonding capacity, despite having substantial swelling. Because the mercerized pulps lack an organized fibrillar structure and thus do not fibrillate, fiber bonding is not increased in refining. The mercerization causes local damage to fibers (generating kinks) and results in substantially lower zero-span strength. Because the mercerized

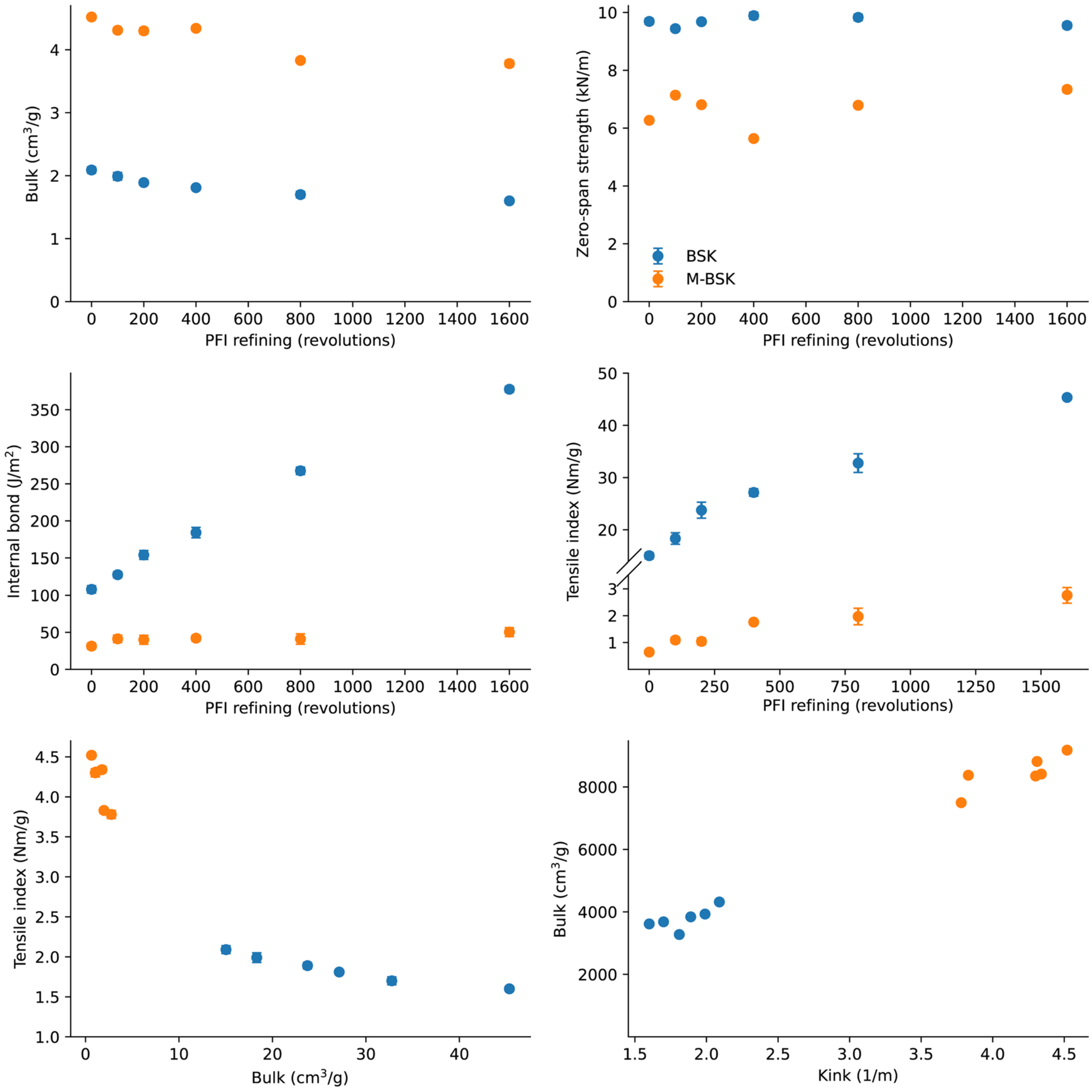

Fig. 6 Mechanical properties of handsheet of unrefined and refined BSK and M-BSK

pulp totally lacks bonding capacity, the bulk of these sheets is greatly elevated. Refining decreased bulk of the mercerized pulp sheets and increased tensile index and internal bond, tensile index increasing from 0.6 to 2.8 Nm/g and internal bond from 31.4 to 50.4 J/m^2 (Fig. 6).

Mercerization of pulp causes a dramatic loss in interfiber bonding capacity. Furthermore, mercerized pulp is unable to effectively fibrillate and increase bonding ability in mechanical refining. It is sometimes speculated that the loss in bonding is due to the extraction of hemicelluloses (Pere et al. 2019). While this may be a contributing factor, most of the hemicellulose was preserved in the pulp in the present study. It seems unlikely that reduction in hemicellulose from 18.7 to 14.0% can explain complete loss in interfiber bonding. Increased curl and kinking of fibers are other factors that can affect fiber packing and bonding, as is seen in Fig. 6, where a correlation is established between tensile index and pulp, and bulk and fiber kink. It seems regenerated cellulose in the mercerized fibers is not able to form interfiber bonds between fibers to nearly the same extent as the cellulose I in untreated fibers. In addition to increased bulk due to fiber kinking, this may be related to the loss is fibrillar structure and changes to the internal changes to the internal hydrogen bonding pattern when fibers are mercerized. This phenomenon is certainly worthy of more detailed study.

Conclusions

The effects of mercerization on refinability, bonding and swelling properties of kraft pulp was studied. Alkaline treatment caused cellulose I to convert to cellulose II and amorphous cellulose and reduced the hemicellulose content from 18.7 to 14.0%. Kinks and external fibrils were introduced in mercerization and the WRV increased slightly. Mercerization increased the microporosity and hydrated surface area of the pulp substantially which is likely related to an increase in amorphous cellulose content.

When the untreated pulp is refined, the fibers swell, fibrillate, and increase the handsheet bonding and strength. However, when mercerized pulp was refined the pulp did not increase in swelling, nor internally or externally fibrillate. It appears that the cell wall of mercerized pulp is internally bonded to such an extent that it cannot loosen and swell by the mechanical treatments used in this study. The refined mercerized fibers have very low bonding capacity and produce a weak, bulky sheet. Mercerized fibers have a curly and kinky morphology which inhibits formation of strong intrafibrillar bonds. Additionally, the low bonding and poor refinability of mercerized pulp are likely related to low bonding of the regenerated cellulose, a largely destroyed microfibrillar structure, and loss of hemicellulose.

Acknowledgments This work made use of Aalto University Bioeconomy Facilities.

Author contributions A.K. wrote the main manuscript, conducted the analysis, and prepared most figures. H.W. performed the measurements, confirmed the results, prepared Fig. 1, and reviewed the final draft. E.H. conceptualized the handsheet strength trials, reviewed the results and the manuscript. T.V. reviewed and edited the manuscript. T.M. developed the concept and designed the methodology, oversaw the project, contributed to writing, and obtained funding. All authors reviewed and approved the final manuscript.

Funding Open Access funding provided by Aalto University. This work was funded by Aalto University. Author A.K. has received research support from Walter Ahlström Foundation and Finnish Forest Products Engineers' Association.

Data availability No datasets were generated or analysed during the current study.

Declarations

Ethical approval Not applicable.

Competing interests The authors declare no competing interests.

References

Agarwal UP, Reiner RS, Ralph SA (2010) Cellulose I crystallinity determination using FT-Raman spectroscopy: Univariate and multivariate methods. Cellulose 17:721–733. https://doi.org/10.1007/s10570-010-9420-z

Agarwal UP, Ralph SA, Baez C, Reiner RS (2021) Detection and quantitation of cellulose II by Raman spectroscopy. Cellulose 28:9069–9079. https://doi.org/10.1007/s10570-021-04124-x

Akhtar M, Blanchette R, Burnes T (1995) Using Simons stain to predict energy savings during biomechanical pulping. Wood Fiber Sci 27:258–264

Azubuike CP, Rodríguez H, Okhamafe AO, Rogers RD (2012) Physicochemical properties of maize cob cellulose powders reconstituted from ionic liquid solution. Cellulose 19:425–433. https://doi.org/10.1007/S10570-011-9631-Y/TABLES/2

Chen X, Kuhn E, Wang W et al (2013) Comparison of different mechanical refining technologies on the enzymatic digestibility of low severity acid pretreated corn stover.

Bioresour Technol 147:401–408. https://doi.org/10.1016/J.BIORTECH.2013.07.109

Chen C, Duan C, Li J et al (2016) Cellulose (Dissolving Pulp) manufacturing processes and properties: a mini-review. BioResources 11:5553–5564. https://doi.org/10.15376/biores.11.4.5553-5564

Choi KH, Kim AR, Cho BU (2016) Effects of alkali swelling and beating treatments on properties of kraft pulp fibers. BioResources 11:3769–3782. https://doi.org/10.15376/biores.11.2.3769-3782

Choi KH, Kim AR, Cho BU (2018) Manufacture of high bulk paper using alkali swollen kraft pulp. Nord Pulp Paper Res 33:503–511. https://doi.org/10.1515/nprrj-2018-3059

Cuissinat C, Navard P (2006) Swelling and dissolution of Cellulose Part II: Free Floating Cotton and Wood fibres in NaOH –. Water – Addit Syst 19–30. https://doi.org/10.1002/masy.200651202

Dias MC, Mendonça MC, Damásio RAP et al (2019) Influence of hemicellulose content of Eucalyptus and Pinus fibers on the grinding process for obtaining cellulose micro/nanofibrils. Holzforschung 73:1035–1046. https://doi.org/10.1515/HF-2018-0230

Dou X, Tang Y (2017) The influence of cold caustic extraction on the purity, accessibility and reactivity of dissolving-grade pulp. ChemistrySelect 2:11462–11468. https://doi.org/10.1002/slct.201701551

Eronen P, Österberg M, Jääskeläinen AS (2009) Effect of alkaline treatment on cellulose supramolecular structure studied with combined confocal Raman spectroscopy and atomic force microscopy. Cellulose 16:167–178. https://doi.org/10.1007/s10570-008-9259-8

Friebel C, Bischof RH, Schild G et al (2019) Effects of caustic extraction on properties of viscose grade dissolving pulp. Processes 7:1–12. https://doi.org/10.3390/pr7030122

Gehmayr V, Potthast A, Sixta H (2012) Reactivity of dissolving pulps modified by TEMPO-mediated oxidation. Cellulose 19:1125–1134. https://doi.org/10.1007/s10570-012-9729-x

Gharehkhani S, Sadeghinezhad E, Kazi SN et al (2015) Basic effects of pulp refining on fiber properties—A review. Carbohydr Polym 115:785–803. https://doi.org/10.1016/J.CARBPOL.2014.08.047

Halonen H, Larsson PT, Iversen T (2013) Mercerized cellulose biocomposites: a study of influence of mercerization on cellulose supramolecular structure, water retention value and tensile properties. Cellulose 20:57–65. https://doi.org/10.1007/S10570-012-9801-6/TABLES/3

Han J, Zhou C, French AD et al (2013) Characterization of cellulose II nanoparticles regenerated from 1-butyl-3-methylimidazolium chloride. Carbohydr Polym 94:773–781. https://doi.org/10.1016/J.CARBPOL.2013.02.003

Hirai A, Tsuji M, Horii F (1997) COMMUNICATION: culture conditions producing structure entities composed of cellulose I and II in bacterial cellulose. Cellulose 4:239–245. https://doi.org/10.1023/A:1018439907396

Hult EL, Larsson PT, Iversen T (2001) Cellulose fibril aggregation — an inherent property of kraft pulps. Polym (Guildf) 42:3309–3314. https://doi.org/10.1016/S0032-3861(00)00774-6

Isogai A, Atalla RH (1998) Dissolution of cellulose in aqueous NaOH solutions. Cellulose 5:309–319

Janson J (1970) Calculation of the polysaccharide composition of wood and pulp. Pap Puu 52:323–328

Ji Y, Peng Y, Strand A et al (2018) Fiber evolution during alkaline treatment and its impact on handsheet properties. BioResources 13:7310–7324. https://doi.org/10.15376/biores.13.4.7310-7324

Jin Z, Wang S, Wang J, Zhao M (2012) Effects of plasticization conditions on the structures and properties of cellulose packaging films from ionic liquid [BMIM]cl. J Appl Polym Sci 125:704–709. https://doi.org/10.1002/APP.34975

Kihlman M, Medronho BF, Romano AL et al (2013) Cellulose dissolution in an alkali based solvent: influence of additives and pretreatments. J Braz Chem Soc 24:295–303. https://doi.org/10.5935/0103-5053.20130038

Koistinen A, Phiri J, Kesari KK et al (2023) Effect of pulp prehydrolysis conditions on dissolution and regenerated cellulose pore structure. Cellulose 30:2827–2840. https://doi.org/10.1007/s10570-023-05050-w

Korhonen O, Budtova T (2019) Gelation of cellulose-NaOH solutions in the presence of cellulose fibers. Carbohydr Polym 224:115152. https://doi.org/10.1016/j.carbpol.2019.115152

Koskenhely K (2008) Refining of chemical pulp fibres. In: Paulapuro H (ed) Papermaking Part 1, Stock Preparation and Wet End, 2nd edn. Finnish Paper Engineers' Association/Paperi ja Puu Oy, Helsinki, pp 94–139

Krässig HA (1993) Cellulose - structure, accessibility and reactivity. Gordon and Breach Science

Kwok TT, Fogg DN, Realff MJ, Bommarius AS (2017) Applying Direct Yellow 11 to a modified Simons' staining assay. Cellulose 24:2367–2373. https://doi.org/10.1007/s10570-017-1269-y

Langan P, Nishiyama Y, Chanzy H (2001) X-ray structure of mercerized cellulose II at 1 Å resolution. Biomacromolecules 2:410–416. https://doi.org/10.1021/bm005612q

Le Moigne N, Jardeby K, Navard P (2010) Structural changes and alkaline solubility of wood cellulose fibers after enzymatic peeling treatment. Carbohydr Polym 79:325–332. https://doi.org/10.1016/j.carbpol.2009.08.009

Li J, Liu X, Zheng Q et al (2019) Urea/NaOH system for enhancing the removal of hemicellulose from cellulosic fibers. Cellulose 26:6393–6400. https://doi.org/10.1007/s10570-019-02587-7

Liu W, Yang L, Lv X (2015) High-permeability Filter Paper prepared from pulp Fiber treated in NaOH/Urea/Thiourea system at low temperature. BioResources 10:5620–5632

Lund K, Sjöström K, Brelid H (2012) Alkali extraction of kraft pulp fibers: influence on fiber and fluff pulp properties. J Eng Fiber Fabr 7:30–39. https://doi.org/10.1177/155892501200700206

Maloney T (2015) Thermoporosimetry of hard (silica) and soft (cellulosic) materials by isothermal step melting. J Therm Anal Calorim 121:7–17. https://doi.org/10.1007/s10973-015-4592-2

Maloney T, Paulapuro H (1999) The formation of pores in the cell wall. J Pulp Pap Sci 25:430–436

Ngene GI, Roux JC, Lachenal D (2022) Xylan extraction strategies and the performance of the resulting high purity cellulose fiber to swelling and dissolution. Carbohydr Polym

Technol Appl 3:100196. https://doi.org/10.1016/j.carpta.2022.100196

Nishiyama Y, Langan P, Chanzy H (2002) Crystal structure and hydrogen-bonding system in cellulose Iβ from synchrotron X-ray and neutron fiber diffraction. J Am Chem Soc 124:9074–9082. https://doi.org/10.1021/ja0257319

Page DH (1989) The beating of chemical pulps – The action and the effects. In: Baker CF, Punton V (eds) Trans. of the IXth Fund. Res. Symp. Cambridge, 1989. Fundamental Research Committee (FRC), Manchester, pp 1–38

Pere J, Pääkkönen E, Ji Y, Retulainen E (2019) Influence of the hemicellulose content on the fiber properties, strength, and formability of handsheets. BioResources 14:251–263. https://doi.org/10.15376/biores.14.1.251-263

Pönni R, Pääkkönen T, Nuopponen M et al (2014) Alkali treatment of birch kraft pulp to enhance its TEMPO catalyzed oxidation with hypochlorite. Cellulose 21:2859–2869. https://doi.org/10.1007/s10570-014-0278-3

Reyes G, King AWT, Koso TV et al (2022) Cellulose dissolution and gelation in NaOH(aq) under controlled CO2 atmosphere: supramolecular structure and flow properties. Green Chem 24:8029–8035. https://doi.org/10.1039/d2gc02916b

Schild G, Sixta H (2011) Sulfur-free dissolving pulps and their application for viscose and lyocell. Cellulose 18:1113–1128. https://doi.org/10.1007/s10570-011-9532-0

Sisson WA (1938) The existence of mercerized cellulose and its orientation in Halicystis as indicated by x-ray diffraction analysis. Science (1979) 87:350. https://doi.org/10.1126/science.87.2259.350

Sluiter A, Hames B, Ruiz RO et al (2011) Determination of structural carbohydrates and lignin in biomass. Laboratory Analytical Procedure (LAP)

Sobue H, Kiessig H, Hess K (1939) Das System cellulose–natriumhydroxyd–wasser in Abhängigkeit Von Der Temperatur. Z fÃ¼r Phys Chem 43B:309–328. https://doi.org/10.1515/zpch-1939-4324

Wada M, Ike M, Tokuyasu K (2010) Enzymatic hydrolysis of cellulose I is greatly accelerated via its conversion to the cellulose II hydrate form. Polym Degrad Stab 95:543–548. https://doi.org/10.1016/j.polymdegradstab.2009.12.014

Wang X, Paulapuro H, Maloney TC (2005) Chemical pulp refining for optimum combination of dewatering and tensile strength. Nord Pulp Paper Res J 20:442–447. https://doi.org/10.3183/npprj-2005-20-04-p442-447

Wohlert M, Benselfelt T, Wågberg L et al (2022) Cellulose and the role of hydrogen bonds: not in charge of everything. Cellulose 29:1–23. https://doi.org/10.1007/s10570-021-04325-4

Yu X, Minor JL, Atalla RH (1995) Mechanism of action of Simons' stain. Tappi J 78:175–180

Yue Y, Han G, Wu Q (2013) Transitional properties of cotton fibers from cellulose I to cellulose II structure. BioResources 8:6460–6471

Zhang S, Wang WC, Li FX, Yu JY (2013) Swelling and dissolution of cellulose in NaOH aqueous solvent systems. Cellul Chem Technol 47:671–679